Cite this as:
P. Niehoff, P. Ebbinghaus, P. Keil, A. Erbe: *Applied Surface Science*, **258**, 3191-3196 (**2012**).

Final copy-edited version of the manuscript is available from:
http://dx.doi.org/10.1016/j.apsusc.2011.11.062

Monolayer formation of Octyltrimethoxysilane and 7-Octenyltrimethoxysilane on silicon(100) covered with native oxide

Philip Niehoff[1], Petra Ebbinghaus, Patrick Keil[2], Andreas Erbe*

[a]*Max-Planck-Institut für Eisenforschung GmbH, Department of Interface Chemistry and Surface Engineering, Max-Planck-Str. 1, 40237 Düsseldorf, Germany*

Abstract

Modification have been carried out of silicon (100) covered with native oxides with monolayers of octyltrimethoxsilane (C8TMS) and octenyltrimethoxysilane (C8enTMS). Different conditions of adsorption from the organic solvents chloroform, toluene and *n*-hexane with subsequent exposure to ammonia vapour under ambient atmosphere have been tested for monolayer formation without exclusion of moisture. Thickness of resulting adsorbates have been measured using spectroscopic ellipsometry (SE), water contact angles were measured, and the surface roughness was determined by atomic force microscopy (AFM). If all three results are consistent with the presence of monolayers on the surface, further characterisation has been carried out by angle dependent X-ray photoelectron spectroscopy (XPS). For monolayers, surface roughnesses about < 0.3 nm were measured, which were mainly determined by the substrate. Thicknesses obtained from SE and XPS agree. Conformational and orientational order of the monolayers determined by attenuated total reflection infrared (ATR-IR) spectroscopy show disordered chains in both cases with nearly isotropic orientation. C8enTMS was found to be partly hydroxylated when treated under alkaline

*Corresponding author; Phone: +49 211 6792 890, Fax: +49 211 6792 218

Email addresses: Philip.Niehoff@uni-muenster.de, Philip.Niehoff@mytum.de (Philip Niehoff), a.erbe@mpie.de, aerbe@arcor.de (Andreas Erbe)

[1]Current address: University of Münster, Institut für Physikalische Chemie, Correnstr. 46, 48149 Münster, Germany

[2]Current address: BASF Coatings GmbH, Glasuritstraße 1, 48165 Münster, Germany

conditions.

Keywords: silane monolayer, vinyl-terminated monolayer, multilayer, surface characterisation

---

1. Introduction

Alkoxy silanes of the type R_x-Si$(OR^{(2)})_{4-x}$, mostly with $x = 1$, have been used extensively to modify hydroxylated surfaces, including oxidic surfaces. Many applications so far have focused on the hydrophobization of silica for use in chromatography [1, 2], or as adhesion promoters [3, 4, 5]. Alkoxy silanes can be applied to modify on hydroxide terminated oxide surfaces, as most relevant for many large scale applications, e.g. on steels, zinc, copper, aluminium, but also on silicon, which is relevant for electronics and nanofluidics applications.

For protection of engineering materials against corrosive attacks from the environment, a variety of coating systems are used. A crucial part here is adhesion between polymer coatings and the native oxides on the metals. To enhance adhesion, molecules with more than one kind of reactive functionality are needed, as they offer the possibility to form covalent bonds with different species. Amongst others, vinyl-terminated alkoxysilanes are one such class of materials [6]. Furthermore, vinyl-terminated silanes offer a starting point for a chemical route for further surface modification [7].

Compared to thiols, which are used for modification of free metal surfaces, the silane's surface chemistry is more complicated, as they can condense without the presence of surface functional groups [8]. Such condensation can be avoided using silanes with only a single Si-O bond [9]. The presence of water in certain amounts is needed to ensure formation of bonds to the surface [1]. However, in large scale applications, the amount of interface water is usually difficult to control.

In the case of adhesion promotion for thick organic coatings, the exact structure of the silane layer is of minor importance [10]. For a further chemical modification aiming at thin, closed organic coatings with a thickness of few

nanometres, a monolayer film, instead of multilayers, is highly desirable. Even though previous studies have been carried out e.g. polymerising from an oxide covered-surface, not much attention has been paid to the actual structure of the molecules on the surface prior to further modification [11].

Chlorosilanes can be used instead of alkoxysilanes to form well-defined monolayers on silicon [12, 13, 14]. The use of a chemistry free of chlorine is, however, advantageous for corrosion protection and in the view of environmental aspects.

Also for alkoxysilane, numerous studies exist in the literature about the structure of silane monolayers with saturated alkyl chains on different surfaces for numerous applications [2, 4, 13, 15, 16, 17, 18, 19]. On the other hand, only few works deal with systems including double bonds [7, 6, 20]. These works all take great care to exclude the presence of moisture.

Recently, a method has been reported to obtain ultrasmooth monolayers of octadecyltrimetoxysilane (C18TMS) [21]. Inspired from this protocol, a comparison is carried out of the ability to form such monolayers between two different silanes, *n*-octyltrimethoxysilane (C8TMS) and 7-octenyltrimethoxysilane (C8enTMS) on silicon with a native oxide. The silicon native oxide here is regarded as a model for other native oxides. The main emphasis will be on the establishment of the formation of monolayers, as opposed to less well-defined adsorbate structures including multilayers while working under conditions which do not exclude moisture.

More precisely, alkoxysilanes can be used to modify silica particles e.g. in aqueous alcoholic solutions [22]. That implies that the condensation of the silanes in the abscence of catalysts of the condensation is slow even in the presence of water. The idea of the protocol used here is as follows. Initially, there is a hydrophilic SiO_2 surface. From the solution in different solvents, silanes can physisorb to the Si wafer. The hydrophilic surface is thought to ensure a driving force for ordered film formation in solvents with low polarity. After removal from solution, exposure to basic ammonia vapour catalyses the transformation from Si-OCH_3 moieties to silanol groups (Si-OH), the presence of which will trigger a subsequent condensation of the silanes. The condensation

leads to formation of bonds to the surface, and to a formation of Si-O-Si of bonds within the monolayer. In a final cleaning step, excess base, water, and loosly bound material is removed from the now modified surface.

In this work, initially, different solvents and reaction conditions have been screened for monolayer formation by spectroscopic ellipsometry (SE), contact angle (CA) measurements and a determination of the surface roughness using atomic force microscopy (AFM). After the formation of monolayers was established, the structures of these monolayers have been studied in detail using X-ray photoelectron spectroscopy (XPS), including angular-resolved measurements, and attenuated total reflection infrared (ATR-IR) spectroscopy.

2. Experimental details

2.1. Materials and preparation

For layer formation experiments, single side polished p-doped silicon wafers (Si-Mat, Germany) of 500 to 550 μm thickness with a resistivity 10–20 Ω cm were cut into pieces of $2 \cdot 1.5$ cm^2. Surfaces were cleaned by 15 min ultrasonication in 2 % alkaline Extran lab detergent (VWR), extensive rinsing with distilled water, and 15 min ultrasonication in 2-propanol (HPLC grade, VWR), before they were dried in a nitrogen stream.

For surface modification, a modification of a published protocol was used [21]. Solvents used to dissolve the silanes were chloroform (HPLC grade; water content <0.05%), *n*-hexane (pro analysis; water content <0.01%), and toluene (Secco Solv dried; water content <0.005%). All solvents were purchased from VWR, and used as received. The water contents given is according to specifications. Samples were dipped into a solution of C8TMS (97%), C8enTMS (95%) or C18TMS (90%) (ABCR, Germany) with respective concentration (2 mM or 10 mM) for a certain time, then dried from the solvent, and finally exposed overnight to the vapour of a concentrated aqueous ammonia solution (pro analysis grade, VWR). Finally, the samples were rinsed with ultrapure water and

then dried using a nitrogen stream. This rinsing step was repeated before every measurement.

The ATR crystals used here were cut from double side polished, N-type Boron-doped silicon wafers of a thickness of 0.5 mm (Si-Mat). The rectangular pieces with dimensions 52*20*0.5 mm^3 were polished on the short sides at an angle of 45° to be used in the ATR setup and cleaned and modified as mentioned above.

2.2. Measurements

SE measurements were carried out with a spectroscopic ellipsometer SE 800 (SENTECH Instruments GmbH, Germany). The light source was a xenon lamp. All SE measurements in this work were done out under an angle of incidence of 70°. To determine the thickness d of the monolayer, the thickness of the native oxide layer on every sample was determined before the modification of the surface with an organic layer. This initial determination is crucial, as there are slight changes in the layer thickness of the oxide between different wafers, and organic materials are almost isorefractive to SiO_2. The experimental data were fit to a model with the following stratification with the real and imaginary parts of the complex refractive index $n + ik$: Air ($n_{\mathrm{air}} = 1.0$)/SiO_2($n_{\mathrm{SiO2}} = 1.452 + \frac{36 \cdot 10^{-4}\ \mathrm{nm}^2}{\lambda^2}$, $k_{\mathrm{SiO2}} = 0$, thickness d_{SiO2} variable)/Si(n_{Si}, k_{Si} according to [23]). After silane treatment, the model used was Air/Organic($n_{\mathrm{organic}} = 1.45$, $k_{\mathrm{organic}} = 0$, d variable)/SiO_2/Si, where all other parameters were the same as for the unmodified surface and d_{SiO2} as determined in the previous experiment was used. Each sample was measured 3 times and was rotated 180° in between.

The topography and root mean square roughness r of the films were investigated by means of AFM using a Dimension 3100 (Digital Instruments, USA). The measurements were carried out using taping mode using a cantilever with a resonant frequency of 300 kHz and a spring constant of 42 N/m (Olympus). The data was processed with Gwyddion using level rows using intersections with given lines.

CA measurements were done with a OCA 20 (dataphysics instruments GmbH,

Germany). Each sample was measured at three different positions with drops of 3 μL. The angle was calculated by Laplace-Young fitting.

XPS (Quantum 2000, Physical Electronics, USA) was measured using a monochromatic Al K_α source at different take-off angles β (15, 20, 45 and 90°) and a pass energy of 23.5 eV. The spectra of the films were measured without any ion sputter cleaning in order to avoid decomposition of the silane layers. Calibration of the binding energy (BE) of the measured spectra was performed by using the energy of the C1s peak (C–C at BE = 285 eV) as an internal reference. The area of the X-ray spot was 100 μm $\times$100μm. Spectra were analysed quantitatively using CasaXPS software.

The intensity at different angles was used to determine the thickness of the deposited monolayers [24, 25]. The integrated intensity I_{C1s} of the C1s peak, which originates exclusively from adsorbed organic layer has been divided by the intensity I_{Si2p} of the Si2p peak, considering the sum of the contribution originating from the bulk Si and SiO_x in the native oxide film. The intensity ratio

$$I^* = \frac{I_{\mathrm{C1s}}}{I_{\mathrm{Si2p}}} \tag{1}$$

is related to d as

$$\ln(I^* + 1) = \frac{d}{\lambda_e \sin(\beta)} + \ln(I_0^*), \tag{2}$$

where I_0^* is an offset and λ_e is the photoelectron mean free path [24, 26, 27]. For alkane monolayers, $\lambda_e = 3.4$ nm [28]. The approach considering the sum of bulk and surface Si is valid here because the difference in mean free path in the respective materials is less than 20%.

A dimensionless quantity ρ proportional to the two-dimensional packing density of molecules on the surface was calculated from the XPS measured at $\beta = 15°$ as

$$\rho = \frac{I_{\mathrm{C1s}} \cdot d_{\mathrm{SiO2}}}{I_{\mathrm{Si2p,\ SiO2}} \cdot d}, \tag{3}$$

with $I_{\mathrm{Si2p,\ SiO2}}$ denoting the intensity of the fraction of SiO_2 of the Si2p peak. While absolute numbers for the packing density are harder to obtain, ρ can be used to compare different samples measured on the same instrument.

For ATR-IR spectroscopy, the Specac 25 Reflections Horizontal ATR accessory (Specac Ltd., Slough, UK) was used. The home-made silicon ATR crystals were fixed by a home-made sample holder pressing only against the edges of the wafer. The measurements were carried out with 1000 scans at a resolution of 2 cm^{-1}. The measurements were done with p- and s-polarisation. The background was obtained by measuring a cleaned, unmodified silicon wafer. Resulting spectra were treated by a bandpass filter to remove high-frequency oscillations from the spectra.

The orientation of the CH_2 groups can be determined from ATR measurements with two perpendicular linear polarisations. The dichroic ratio is directly related to the orientational order parameter

$$S_2 = \frac{3\langle\cos^2\vartheta\rangle - 1}{2} \tag{4}$$

with the tilt angle ϑ between the respective transition dipole moment and the surface normal [29]. Determination of $\langle\vartheta\rangle$ relies on the knowledge of the distribution of tilt angles. In an isotropic system, the distribution is such that $S_2 = 0$.

3. Results and Discussion

3.1. Screening

During the monolayer formation process of a certain silane on an oxide covered silicon surface, several experimental parameters can exert an influence on the structure of the resulting layer. To optimise these parameters, a screening was performed, checking layer thickness, surface roughness and contact angles.

In the screening, different incubation times, silane concentrations and solvents of different polarity (chloroform, *n*-hexane, and toluene) have been tested. The choice of solvents was motivated by the difference in dielectric constant and its effect expected on the silane layer [13]. At room temperature, chloroform has a static dielectric constant of 4.81, toluene of 2.38, and *n*-hexane 1.89 [13].

Contact angles for the layer of C18TMS were found to be above 100° [21]. Perfect monolayer structures of C8TMS are expected reach these values as well.

The layer thickness was screened by ellipsometry. For monolayers of the silanes, the expected value for the layer thickness is between (1.24 ± 0.1) nm and 0 nm. The value of 1.24 nm is the distance between the outermost hydrogen atom and the middle of the silicon-oxygen bond, calculated from molecular models of C8TMS, assuming a chain in all-*trans* conformation. The error of 0.1 nm, determined by multiple measurements of a silicon oxide layer on silicon, is taking the measurement accuracy into account. Furthermore, if an ordered monolayer is formed, the roughness of the sample should be of the same size as the root mean square roughness of the silicon (100) wafer, determined as between 0.12 and 0.35 nm. Layers failing one of the criteria have been discarded for further analysis.

Tables 1 and 2 show the screening results for C8TMS and C8enTMS, respectively.

In the case of C8enTMS for hexane and toluene, d increases with increasing incubation time and concentration. For chloroform, a differentiated behaviour is found. The case of C8TMS shows no systematic results.

Layer thickness bigger than 1.34 nm can be disregarded, as in these cases, multilayers have been formed. C8TMS samples prepared from a 10 mM toluene and 2 mM chloroform solution with an incubation time of 10 min and both concentrations in toluene at 24 h fulfil all required criteria. The 10 min sample shows the higher layer thickness, which could be indicating a more upright orientation, which is why these conditions have been used for further analysis.

For the C8enTMS, according to the thickness criterion of 1.25 nm, three samples fit, samples prepared from 2 mM solutions with 10 min incubation in chloroform and toluene, as well as the sample exposed to 10 mM solution in chloroform for 2 h. Almost all samples show only a rather low contact angle of around 80°. Only the contact angles from chloroform solution after longer incubation times show higher values, with 104 and 88°. But the thicknesses of those samples are too high for a monolayer structure. For these reasons the samples showing the smallest thickness, which are the chloroform, 10 mM and 2 h incubation time samples, were tested for its reproducibility.

	2 mM			10 mM		
	d / nm	r / nm	γ / °	d / nm	r / nm	γ / °
$CHCl_3$, 10 min	*1.3*	-	*99*	1.2	1.43	98
$CHCl_3$, 2 h	0.3	0.1	76	0.6	0.11	73
$CHCl_3$, 24 h	2.0	0.7	80	6.4	0.80	86
n-C_6H_{14}, 10 min	2.3	-	99.4	1.6	-	101
n-C_6H_{14}, 2 h	0.3	0.1	69	1.0	0.3	73
n-C_6H_{14}, 24 h	3.2	0.2	97	3.3	1.9	98
C_6H_5–CH_3, 10 min	0.8	0.2	81	***0.9***	***0.1***	***105***
C_6H_5–CH_3, 2 h	2.9	-	-	2.0	0.2	-
C_6H_5–CH_3, 24 h	*0.5*	*0.2*	-	*0.6*	*0.2*	-

Table 1: Layer thickness d, root mean square (rms) roughness r, and contact angles γ of C8TMS layers prepared with the respective incubation times in chloroform, n-hexane and toluene. Conditions yielding results in italic fulfil the required monolayer criteria, those yielding the bold-face values have been used in later experiments.

	2 mM			10 mM		
	d / nm	r / nm	γ / °	d / nm	r / nm	γ / °
$CHCl_3$, 10 min	*1.1*	*0.3*	*80*	1.8	0.3	81
$CHCl_3$, 2 h	1.6	0.2	104	***1.2***	***0.2***	***81***
$CHCl_3$, 24 h	*1.3*	*0.2*	*88*	2.8	0.2	82
n-C_6H_{14}, 10 min	1.6	0.4	79	2.2	0.4	81
n-C_6H_{14}, 2 h	1.8	0.3	81	2.4	0.5	84
n-C_6H_{14}, 24 h	2.1	0.3	78	3.0	0.3	79
C_6H_5–CH_3, 10 min	*1.2*	*0.3*	*83*	1.4	0.3	80
C_6H_5–CH_3, 2 h	1.4	0.2	82	*1.3*	*0.2*	*80*
C_6H_5–CH_3, 24 h	1.5	0.2	82	1.5	0.2	79

Table 2: Layer thickness d, roughness r, and contact angles γ of C8enTMS layers prepared with the respective incubation times in chloroform, n-hexane and toluene. Conditions yielding results in italic fulfil the required monolayer criteria, those yielding the bold-face values have been used in later experiments.

The layer formation on the samples which yield monolayers matching the above-mentioned criteria was repeatable. For C8TMS from 10 mM toluene and 10 min incubation time $d = (0.9 \pm 0.2)$ nm and $\gamma = (105 \pm 3)°$. The average roughness of these samples are not higher than the ones measured for the silicon samples.

For C8enTMS samples, 2 h incubation in 10 mM silane in $CHCl_3$ was chosen, and $d = 1.2 \pm 0.2$ nm and $\gamma = 81 \pm 1°$. Average roughnesses of the samples were all below or within the roughness range of the silicon wafer itself.

It must be noted that the errors given in the preceding paragraph are errors obtained from the measurement of three samples prepared in the same way, while for individual samples, the errors were obtained by measuring several spots on one sample.

Therefore, for both substances, reproducible formation of layers with monolayer thickness is obtained. Looking at the results obtained, it appears that under the conditions employed here, frequently multilayers are formed from *n*-hexane. What is more striking is the fact that there is no clear trend in the adsorbate structure results with incubation time. In all solvents for C8TMS, the 2 h incubation time sample looks substantially different from both the 10 min and 24 h incubation time sample, indicating a change in layer formation mechanism with time. Such effects are not studied further here, though they require considerable more attention for a complete understanding. The behaviour found here may indicate that self-assembly is not the only factor determining the adsorbate structure.

3.2. In-depth characterisation of monolayers

The structures of monolayers formed where characterised in more detail by AFM, angle-dependent XPS and ATR-IR spectroscopy.

Figures 1a and 1b show AFM images of the surfaces after surface modification. In both cases, the rms roughness is on the scale of 0.2 nm over an area of several μm. The roughness does not change upon surface modification. The stripe pattern visible on the modified surfaces is an imaging artifact, as it was

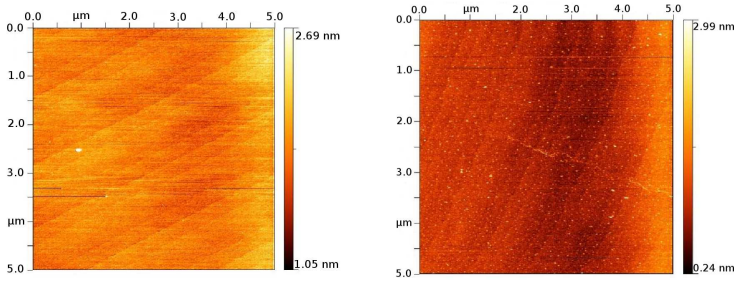

(a) (b)

Figure 1: AFM images of (a) C8TMS and (b) C8enTMS monolayers on Si.

found to orient differently for different scans of the same sample with the same scan direction.

XP spectra of C8TMS monolayers, displayed in 2a and 2b show the presence of only one kind of carbon on the surface. In the case of C8enTMS, the C1s region of the XP spectrum shows the presence of two peaks at all angles of incidence. The major contribution is in the peak at 285.0 eV, assigned to carbon in CC (including single and double bonds) and CH bonds [30]. The second peak, with an intensity of 5 % of the peak of aliphatic carbon is centred around 286.7 eV, is assigned to carbon in C-O bonds [30].

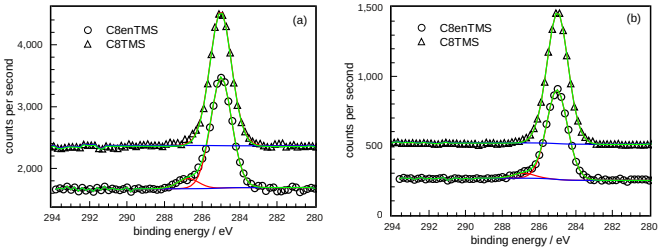

Figure 2: C1s region of XP spectra of C8TMS and C8enTMS on silicon at (a) $\beta = 90°$ and (b) $\beta = 20°$, together with peak fits. The curves for C8TMS have been offset for clarity.

Further insight into the surface structure can be obtained by comparing the

packing densities of the C8TMS and the C8enTMS samples. Here $\rho \sim (3.2 \pm 0.5)$ for C8TMS and $\rho \sim (2.5 \pm 0.4)$ for C8enTMS were obtained. Due to the relatively large error, which mainly originates from the 20% error of d, no safe statements can be made whether the packing density for C8TMS is higher than that for C8enTMS.

The difference in the chemical composition between C8TMS and C8enTMS modified surfaces is manifested in the ATR-IR spectra, which are displayed in Figure 3. Both monolayers show the characteristic antisymmetric and symmetric stretching modes of methylene groups at 2926 and 2856 cm^{-1}, respectively [31, 32, 29]. C8TMS monolayers show in addition stretching modes of methyl groups at 2962 and 2878 cm^{-1}. C8enTMS monolayers do not show these modes, as they do not contain methyl groups. The latter samples do, however, show a small peak at 3012 cm^{-1}, which could be interpreted as originating from CH stretching modes of unsaturated chains.

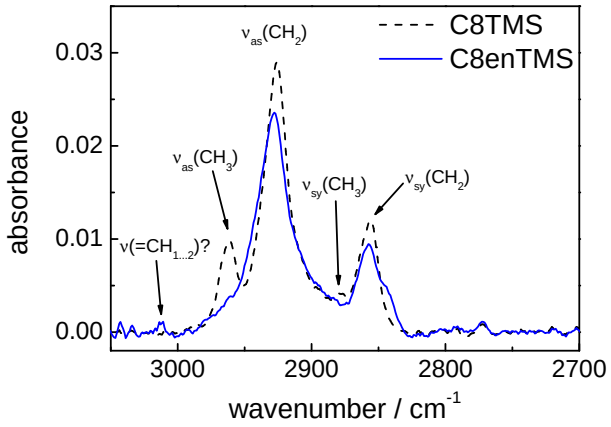

Figure 3: ATR-IR spectra of C8TMS and C8enTMS modified silicon surfaces.

The XPS results show the presence of oxygen in the C8enTMS layers. This presence is interpreted as originating from partial base-catalysed addition of water to the C=C bond. This finding is also explaining the observation that

despite an expected hydrophobic modification of the surface, contact angles of C8enTMS are $\sim 20°$ lower than at C8TMS monolayers. As in total 25 % of the carbon atoms are expected to be in C=C double bounds, and water addition to the double bonds yields one atom with C-O bond, an estimate based on the peak area shows that about one third of the C=C bonds are modified in the resulting layers. A control experiment subjecting the layers to alkaline treatment shows a further significant increase in the number C-O bonds.

The thickness determination carried out above by spectroscopic ellipsometry rely on an accurate estimate of the refractive index of the layer. A second method to determine the thickness of a layer is the analysis of the intensities of XPS data measured at different β [26, 27]. Results for three samples are shown in Figure 4. From the slope of these plots, a layer thickness d_{XPS} is estimated as described above. For C8TMS, $d_{\mathrm{XPS}} \sim (0.8 \pm 0.1)$ nm, while the thickness determined by ellipsometry for the same sample was found to be (1.0 ± 0.1) nm. For C8enTMS, $d_{\mathrm{XPS}} \sim (0.7 \pm 0.1)$ nm with an ellipsometric thickness of (1.1 ± 0.1) nm. In both cases, the ellipsometric thickness is slightly higher than XPS thickness. For reference, a sample with a C18TMS monolayer showed $d_{\mathrm{XPS}} \sim (1.5 \pm 0.2)$ nm.

More information about the internal structure of the chains in the silane monolayers can be obtained from closer inspection of the CH_2 stretching modes in the IR spectra. For C8TMS, the maxima of the antisymmetric and symmetric CH_2 stretching modes are 2926 and 2856 cm^{-1}, respectively, while for C8enTMS, they are 2927 and 2857 cm^{-1}. These frequencies are indicative of disordered chains with many *gauche* conformers [31, 32]. Interestingly, in the C8enTMS spectra, the symmetric stretching mode shows a shoulder with a maximum below 2850 cm^{-1}. This second population is rarely observed in spectra and could hint to a certain fraction of ordered chains in all-*trans* conformation [31, 32].

The analysis of the dichroic ratio here yields values of S_2 between -0.15 and 0.05, leaving room for interpretation. The system may either be nearly isotropic with upright oriented chains in slight excess, or it may be highly ordered with

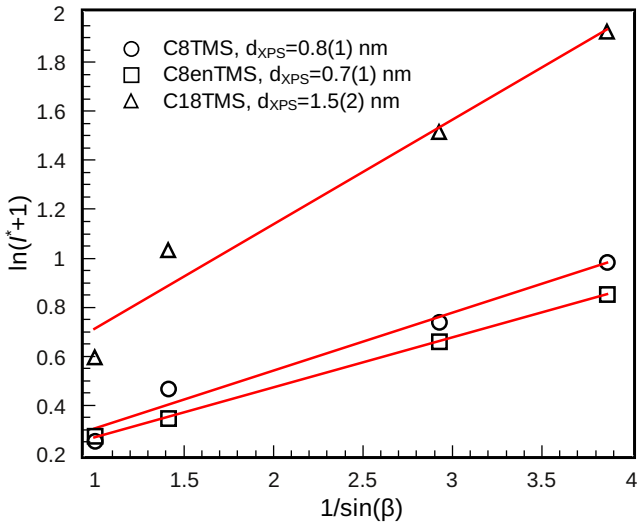

Figure 4: Analysis of I^* from XPS measurements at different β for C8TMS and C8enTMS. For comparison, results for C18TMS is also shown.

chains of $\vartheta \sim 54°$. The absence of conformational order, as indicated by the high frequencies of the CH_2 stretching modes, favours the former interpretation. The average orientation of the chain elements with respect to the surface normal is about $(47 \pm 5)°$.

3.3. Comparison

For C8TMS, chains with a large conformational order have been found when the preparation is done at sufficiently low temperature ($< 10°$C) [14]. On the other hand, C18TMS, shows ordered chains already when prepared at room temperature [14, 21], and disorder is found when preparing $> 30°$C [14]. Here, temperature dependence has not been investigated, however, the findings here confirm the statements made before. Nevertheless, the monolayers prepared here are extremely smooth, comparably in roughness to ordered C18TMS [21].

The fact that disorder in the chains is observed can be understood when inspecting the local bonding situation on the surfaces. Due to the distance between the chains, which are given by the distance between two silanol groups

on the surface, voids between the chains are created, which can be filled by introducing few gauche conformers in the chains.

3.4. Chemical reactivity of the surfaces

The layer of C8enTMS on silicon (100) was tested for its chemical reactivity. Since all double bonds should be located at the air/solid interface, further chemical modification of the formed monolayers should be possible. This was tested by subjecting some C8enTMS monolayer to an alkaline treatment at pH 11, followed by 2 h ultrasonication. Under these conditions, a hydroxylation of the C=C bond is possible. For comparison, the same treatment has been imposed on C8TMS samples. C8TMS samples show no change in d and γ after the treatments. C8enTMS samples show an increase in d by 0.4 nm and a $\sim 20°$ reduction in γ. XPS analysis of the samples after treatment show an increase of the C-O fraction under the C1s peak at 287 eV by a factor of 2-3 compared to the untreated surface. While increase in C-O fraction and decrease in contact angle are expected, the increase in layer thickness is not, and is probably only an apparent increase originating from the fact that hydroxylation of the monolayer leads to a larger affinity for water adsorption. This hypothesis is in agreement with the film thickness measured in ultra-high vacuum by angular resolved XPS, which was found to be (0.7 ± 0.2) nm before and after the treatment.

4. Conclusions

Smooth monolayers of both C8TMS and C8enTMS monolayers have been prepared from toluene and chloroform solution, respectively. From n-hexane solutions, resulting adsorbate structures are not monolayers. Under the conditions needed for monolayer preparation, C8TMS monolayers show an ellipsometric layer thickness of (0.9 ± 0.2) nm and a contact angle of 105°, and a layer thickness from angle-dependent XPS of (0.8 ± 0.1) nm. ATR-IR spectroscopic studies show conformationally disordered chains with a tilt angle of the average chain segment around one CH_2 group near the angle expected for isotropic orientation. C8enTMS monolayers show an ellipsometric thickness of (1.2 ± 0.2)

nm, and a contact angle of 81°. XPS results give a slightly lower layer thickness of (0.7 ± 0.1) nm. Alkaline treatment leads to addition of water to the double bond. Other chemical modifications can be performed on the double bond. No essential difference in the structure of the saturated and ω-unsaturated monolayer were found here. These results imply that the use of saturated silanes as models for adhesion promoters with other functionalities in the chain are supposed to produce valid results.

References

[1] E. Vansant, P. van der Voort, K. Vrancken, Characterization and chemical modification of the silica surface, volume 93 of *Studies in Surface Science and Catalysis*, Elsevier, Amsterdam, 1997.

[2] P. van der Voort, E. F. Vansant, J. Liq. Chrom. Rel. Technol. 19 (1996) 2723–2752.

[3] K. Mittal, Silanes and Other Coupling Agents, VSP, Utrecht, 1992.

[4] G. L. Witucki, D. Corning, J. Coat. Technol. 65 (1993) 57–60.

[5] Y. Xie, C. A. Hill, Z. Xiao, H. Militz, C. Mai, Compos. A: Appl. Sci. Manuf. 41 (2010) 806–819.

[6] L. Vast, J. Delhalle, Z. Mekhalif, Int. J. Adhes. Adhesives 29 (2009) 286–293.

[7] T. Miyake, T. Tanii, K. Kato, T. Hosaka, Y. Kanari, H. Sonobe, I. Ohdomari, Chem. Phys. Lett. 426 (2006) 361–364.

[8] M. Kind, C. Wöll, Prog. Surface Sci. 84 (2009) 230–278.

[9] Y. Wen, W. Yi, L. Meng, M. Feng, G. Jiang, W. Yuan, Y. Zhang, H. Gao, L. Jiang, Y. Song, J. Phys. Chem. B 109 (2005) 14465–14468.

[10] G. Tillet, B. Boutevin, B. Ameduri, Prog. Polym. Sci. 36 (2011) 191–217.

[11] K. O. Siegenthaler, A. Schäfer, A. Studer, J. Am. Chem. Soc. 129 (2007) 5826–5827.

[12] B. Wu, G. Mao, K. S. Ng, Colloids Surf. A: Physicochem. Eng. Aspects 162 (1999) 203–213.

[13] T. Manifar, A. Rezaee, M. Sheikhzadeh, S. Mittler, Appl. Surf. Sci. 254 (2008) 4611–4619.

[14] D. H. Lee, T. Oh, K. Cho, J. Phys. Chem. B 109 (2005) 11301–11306.

[15] A. Wang, H. Tang, T. Cao, S. O. Salley, K. S. Ng, J. Colloid Interface Sci. 291 (2005) 438–447.

[16] D. H. Kim, H. S. Lee, H. Yang, L. Yang, K. Cho, Adv. Funct. Mater. 18 (2008) 1363–1370.

[17] S. A. Kulkarni, K. P. Vijayamohanan, Surf. Sci. 601 (2007) 2983–2993.

[18] I. de Graeve, J. Vereecken, A. Franquet, T. van Schaftinghen, H. Terryn, Prog. Org. Coat. 59 (2007) 224–229.

[19] C. Le Pen, B. Vuillemin, S. Van Gils, H. Terryn, R. Oltra, Thin Solid Films 483 (2005) 66–73.

[20] Y.-S. Li, N. E. Vecchio, Y. Wang, C. McNutt, Spectrochim. Acta A 67 (2007) 598–603.

[21] Y. Ito, A. A. Virkar, S. Mannsfeld, J. H. Oh, M. Toney, J. Locklin, Z. Bao, J. Am. Chem. Soc. 131 (2009) 9396–9404.

[22] T. R. Khan, A. Erbe, M. Auinger, F. Marlow, M. Rohwerder, Sci. Technol. Adv. Mater. 12 (2011) 055005.

[23] J. Geist, D. F. Edwards, in: Handbook of optical constants of solids, volume III, Elsevier, pp. 519–536.

[24] K. M. R. Kallury, J. D. Brennan, U. J. Krull, Anal. Chem. 67 (1995) 2625–2634.

[25] J. He, Z.-H. Lu, S. A. Mitchell, D. D. M. Wayner, J. Am. Chem. Soc. 120 (1998) 2660–2661.

[26] W. Fraser, J. Florio, W. Delgass, W. Robertson, Surf. Sci. 36 (1973) 661–674.

[27] C. Fadley, R. Baird, W. Siekhaus, T. Novakov, S. Bergström, J. Electron Spec. Rel. Phenom. 4 (1974) 93–137.

[28] M. P. Seah, W. A. Deuch, Surf. Interface Anal. 1 (1979) 2–11.

[29] E. Goormaghtigh, V. Raussens, J.-M. Ruysschaert, Biochim. Biophys. Acta (Biomembranes) 1422 (1999) 105–185.

[30] R. Benoit, Y. Durand, B. Narjoux, G. Quintana, http://www.lasurface.com/, 2011.

[31] R. G. Snyder, H. L. Strauss, C. A. Elliger, J. Phys. Chem. 86 (1982) 5145–5150.

[32] R. Macphail, H. Strauss, R. Snyder, C. Elliger, J. Phys. Chem. 88 (1984) 334–341.